

# Intracratonic asthenosphere upwelling and lithosphere rejuvenation beneath the Hoggar swell (Algeria): Evidence from HIMU metasomatised lherzolite mantle xenoliths

L. Beccaluva<sup>a,\*</sup>, A. Azzouni-Sekkal<sup>b</sup>, A. Benhallou<sup>c</sup>, G. Bianchini<sup>a</sup>, R.M. Ellam<sup>d</sup>,  
M. Marzola<sup>a</sup>, F. Siena<sup>a</sup>, F.M. Stuart<sup>d</sup>

<sup>a</sup> *Dipartimento di Scienze della Terra, Università di Ferrara, Italy*

<sup>b</sup> *Faculté des Sciences de la Terre, Géographie et Aménagement du Territoire, Université des Sciences et Technologie Houari Boumédiène, Alger, Algeria*

<sup>c</sup> *CRAAG (Centre de Recherche en Astronomie, Astrophysique et Géophysique), Alger, Algeria*

<sup>d</sup> *Isotope Geoscience Unit, Scottish Universities Environmental Research Centre, East Kilbride, UK*

Received 7 March 2007; received in revised form 23 May 2007; accepted 24 May 2007

Available online 2 June 2007

Editor: R.W. Carlson

## Abstract

The mantle xenoliths included in Quaternary alkaline volcanics from the Manaz-district (Central Hoggar) are proto-granular, anhydrous spinel lherzolites. Major and trace element analyses on bulk rocks and constituent mineral phases show that the primary compositions are widely overprinted by metasomatic processes. Trace element modelling of the metasomatised clinopyroxenes allows the inference that the metasomatic agents that enriched the lithospheric mantle were highly alkaline carbonate-rich melts such as nephelinites/melilitites (or as extreme silico-carbonatites). These metasomatic agents were characterized by a clear HIMU Sr–Nd–Pb isotopic signature, whereas there is no evidence of EM1 components recorded by the Hoggar Oligocene tholeiitic basalts. This can be interpreted as being due to replacement of the older cratonic lithospheric mantle, from which tholeiites generated, by asthenospheric upwelling dominated by the presence of an HIMU signature. Accordingly, this rejuvenated lithosphere (accreted asthenosphere without any EM influence), may represent an appropriate mantle section from which deep alkaline basic melts could have been generated and shallower mantle xenoliths sampled, respectively. The available data on lherzolite xenoliths and alkaline lavas (including He isotopes, Ra <9) indicate that there is no requirement for a deep plume anchored in the lower mantle, and that sources in the upper mantle may satisfactorily account for all the geochemical/petrological/geophysical evidence that characterizes the Hoggar swell. Therefore the Hoggar volcanism, as well as other volcanic occurrences in the Saharan belt, are likely to be related to passive asthenospheric mantle uprising and decompression melting linked to tensional stresses in the lithosphere during Cenozoic reactivation and rifting of the Pan–African basement. This can be considered a far-field foreland reaction of the Africa–Europe collisional system since the Eocene.

© 2007 Elsevier B.V. All rights reserved.

**Keywords:** Hoggar; mantle xenoliths; asthenospheric upwelling; lithosphere/asthenosphere interaction; lithosphere rejuvenation; metasomatism; trace elements; Sr–Nd–Pb isotopes

\* Corresponding author.

E-mail address: [bcc@unife.it](mailto:bcc@unife.it) (L. Beccaluva).

## 1. Introduction

The Cenozoic volcanism of the Hoggar region (Algeria) represents one of the most important magmatic district of the North African belt. It covers more than 10,000 km<sup>2</sup> and is associated with a regional crustal swell of Pan–African terranes, approximately 1000 km in diameter (Fig. 1). The oldest Cenozoic volcanic rocks are represented by a thick pile of tholeiitic plateau basalts (35–30 Ma) that are characterized by an isotopic signature typical of EM1-type enriched mantle (Aït-Hamou et al., 2000). Younger (Neogene–Quaternary) volcanic rocks have a generally alkaline affinity and include both basic lavas and trachyte–phonolite differentiates, with a prevalent HIMU (high  $\mu$ ) Pb–Nd–Sr isotopic signature (Allègre et al., 1981; Azzouni-Sekkal et al., 2007). In the Atakor–Manzaz districts, the latest volcanic episodes are markedly alkaline (basanites and nephelinites) sometimes entraining mantle xenoliths which are the object of this study.

The Cenozoic volcanism appears to be linked to the domal basement uplift of the Hoggar area, and could reflect interaction between the lithosphere and the underlying convecting mantle. This in turn may have important implications for the existence of possible mantle plumes and related geochemical components, as well as for the role played by pre-existing tectonic lineaments of the Pan–African lithosphere.

The mantle xenoliths from the Manzaz district provide important constraints on the compositional evolution of the lithospheric mantle beneath the area and, by implication, on mantle sources from which the Hoggar magmas were generated. Detailed studies of mantle lithologies of the whole North African belt are only reported for the In Teria district, NE Hoggar (Dautria et al., 1992), and more recently for Morocco (Raffone et al., 2001; Raffone et al., 2004) and Libya (Beccaluva et al., in press). In this paper we present new major and trace element analyses of both bulk-rocks and constituent minerals, as well as Sr–Nd–Pb (He) isotopes on separated minerals in order to define the geochemical features of the main metasomatic components, their provenance and role in the North African lithospheric evolution. The results also contribute to a better understanding of the tectono-magmatic setting of the Hoggar volcanism and its origin either from a deep plume (Allègre et al., 1981; Aït-Hamou et al., 2000) or to relatively shallow processes in the upper mantle (Azzouni-Sekkal et al., 2007; Liégeois et al., 2005).

## 2. Petrography, mineral and bulk rock composition

Mantle xenoliths studied in this paper represent a selection of nine representative samples (up to 8–9 cm in size) from a larger xenolith population collected from two scoria cones in the Manzaz volcanic district (N 23°

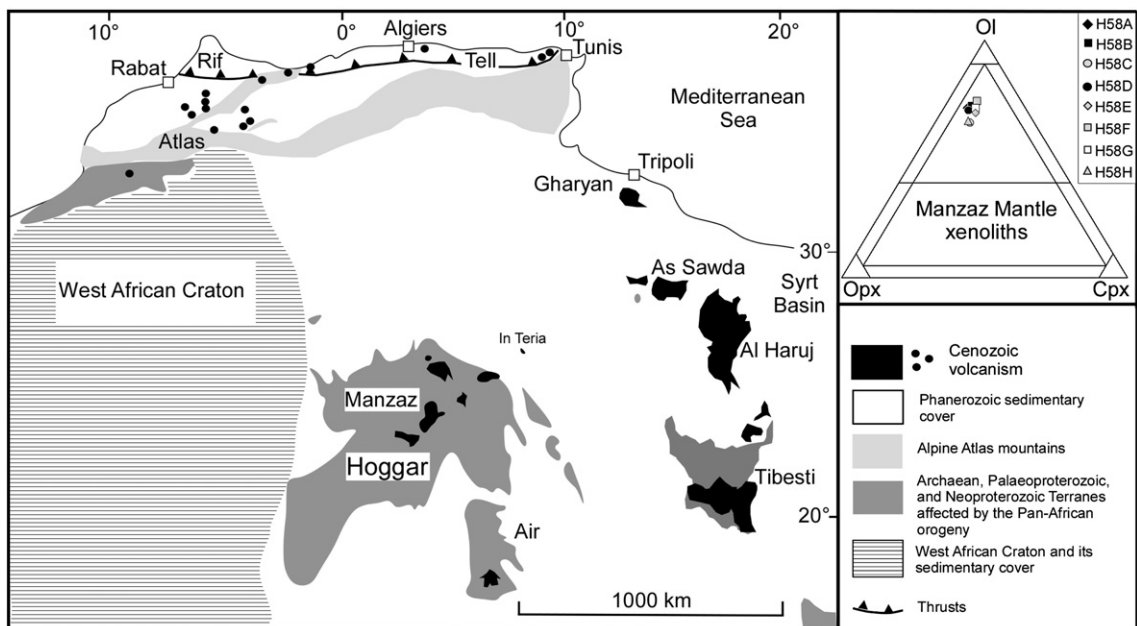


Fig. 1. Sketch map indicating locations of the main Cenozoic volcanic fields of North Africa, after (Liégeois et al., 2005) modified. Modal compositions of the Manzaz mantle xenoliths in terms of olivine (ol), orthopyroxene (opx), clinopyroxene (cpx) are also reported.

49.5' 71''–E 5° 53.7' 20''; N 23° 50.5' 42''–E 5° 50.5' 68''). They are dominantly protogranular to equigranular lherzolites and are characterized by a typical four phase mineral assemblage. They show no evidence of basalt infiltration.

The primary paragenesis in protogranular domains consists of medium sized lobate olivine and orthopyroxene crystals (2–3 mm), and smaller interstitial green clinopyroxene and brown spinel (isodiametric to holly leaf in shape). The largest orthopyroxenes sometimes show clinopyroxene exsolution lamellae. Kink banding is quite frequent in both olivine and orthopyroxene. The evidence of strain and deformation in these crystals, together with the absence of cumulate textures, rules out a cumulate origin for these xenoliths.

Secondary metasomatic textures are scarce and consist of rare spongy rims in clinopyroxene and microcrystalline patches/lenses (particularly in sample H58D) where glass is typically absent. These microdomains are widely obliterated by recrystallization processes leading to equigranular textures, disappearance of unmixing lamellae and development of triple junctions between the undeformed crystals (average grain size less than 1 mm across).

Microprobe analyses showing compositional variations even within individual crystals and in different textural domains are reported in Table 1 in Appendix A of the online supplement and analytical methods in Appendix B.

Olivine (ol) consists of rather homogeneous crystals with Fo ranging between 89.1 and 91.3. Orthopyroxene (opx) composition varies in the following ranges: En 87.2–89.7, Fs 8.8–10.7, Wo 1.2–2.1, with Mg # [Mg/(Mg+Fe)] 0.89–0.91, showing an apparent equilibrium with the coexisting olivine.

Clinopyroxene (cpx) has a wider compositional range: En 46.4–54.6, Fs 4.5–7.1, Wo 38.4–47.7, with Mg # 0.88–0.92, Cr # [Cr/(Cr+Al)] 0.05–0.13, Na<sub>2</sub>O 0.67–1.55 wt.% and TiO<sub>2</sub> 0.17–0.68 wt.%. As observed in Fig. 2 the compositions of these clinopyroxenes appear to be typical of fertile lherzolites (Mysen and Kushiro, 1977; Jaques and Green, 1980), with the relatively more depleted compositions (samples H58A, H58B and H58D) partially overlapping the abyssal peridotite field (Fig. 2a).

Clinopyroxene occurring as spongy rims and/or in re-equilibrated equigranular domains, which are probably related to metasomatic reactions, tends to have comparatively lower Na<sub>2</sub>O and CaO (and higher MgO) contents (Fig. 2b).

Spinel (sp) shows the following compositional range: Mg # 0.75–0.83, Cr # 0.09–0.22, conforming to the compositions typical of fertile mantle peridotites, with

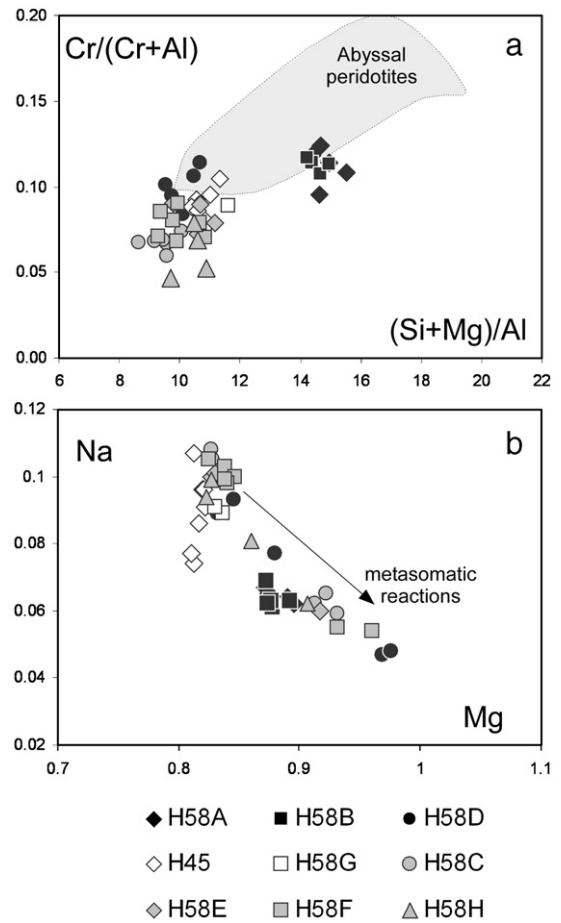


Fig. 2. Cr/(Cr+Al) vs. (Si+Mg)/Al (a) and Na vs. Mg (b) for clinopyroxene from Manazas mantle xenoliths as atoms per formula units (a.f.u.) on the basis of 6 oxygens. In (a) compositional field of abyssal peridotites (Johnson et al., 1990) also reported for comparison.

more refractory compositions (Cr # 0.20–0.22) observed in samples H58A, H58B and H58D.

Application of the two-pyroxene geothermometer (Brey and Köhler, 1990) using the core composition of equilibrated crystals gives nominal equilibration temperatures in the range of 950–1060 °C.

Major element mass balance calculations using mineral phases and whole rock compositions (Table 2 in Appendix A of the online supplement; analytical methods in Appendix B) provide the following modal abundances: 64%–73% ol, 17%–22% opx, 8%–12% cpx, 1–3% sp. As expected, lower cpx modal abundances (8–9%) are recorded in three samples (H58A, H58B and H58D) where the constituent phases have more refractory compositions.

In the Al<sub>2</sub>O<sub>3</sub> and CaO vs MgO diagrams (Fig. 3) the Manazas bulk-rock peridotites are compared with those of other xenolith suites from Cenozoic volcanic

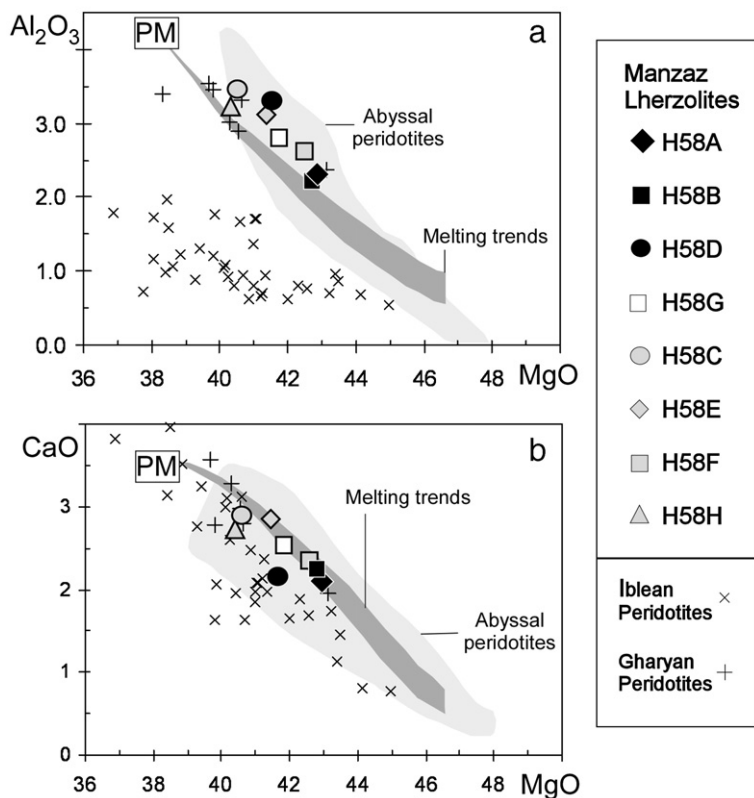


Fig. 3. Bulk rock analyses of Manzaz lherzolite xenoliths in terms of  $Al_2O_3$  vs  $MgO$  (a) and  $CaO$  vs  $MgO$  (b), compared to other mantle xenoliths from the African plate (Gharyan, Libya (Beccaluva et al., in press); Iblean district, SE Sicily (Beccaluva et al., 2005)). The field of abyssal peridotites (light grey) and residual trends after melt extraction (dark grey) from a fertile lherzolite source (PM) after Niu (1997) are also reported.

occurrences in the African plate (Gharyan district, Libya (Beccaluva et al., in press); Iblean district, Sicily (Beccaluva et al., 2005), as well as with abyssal peridotites and theoretical mantle residua after progressive partial melting (Niu, 1997). Comparison with these fields suggests that the Manzaz mantle xenoliths

underwent a moderate depletion related to previous melting processes.

In the chondrite-normalized bulk-rock Rare Earth Elements (REE) patterns of Fig. 4, Manzaz peridotites have heavy (H)REE (Tb–Lu) that range between 1.1–1.2 (H58A and H58B), to 1.8 (H58D), and 2.4 (H58C) ×

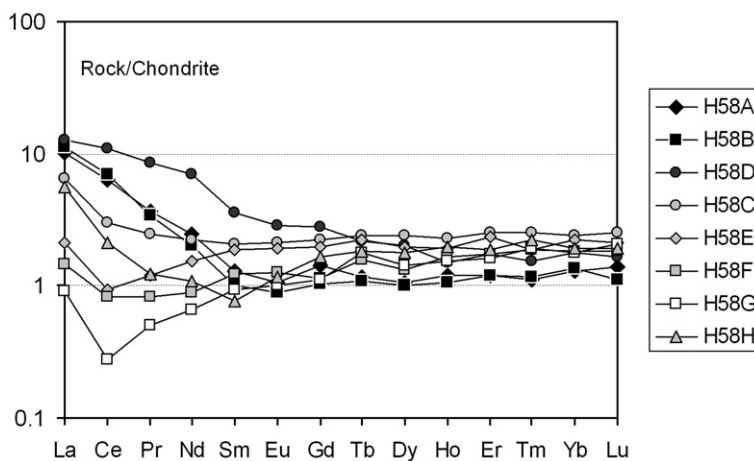


Fig. 4. Chondrite-normalized REE patterns for bulk rock lherzolite xenoliths from Manzaz. Normalizing factors after Sun and McDonough (1989).

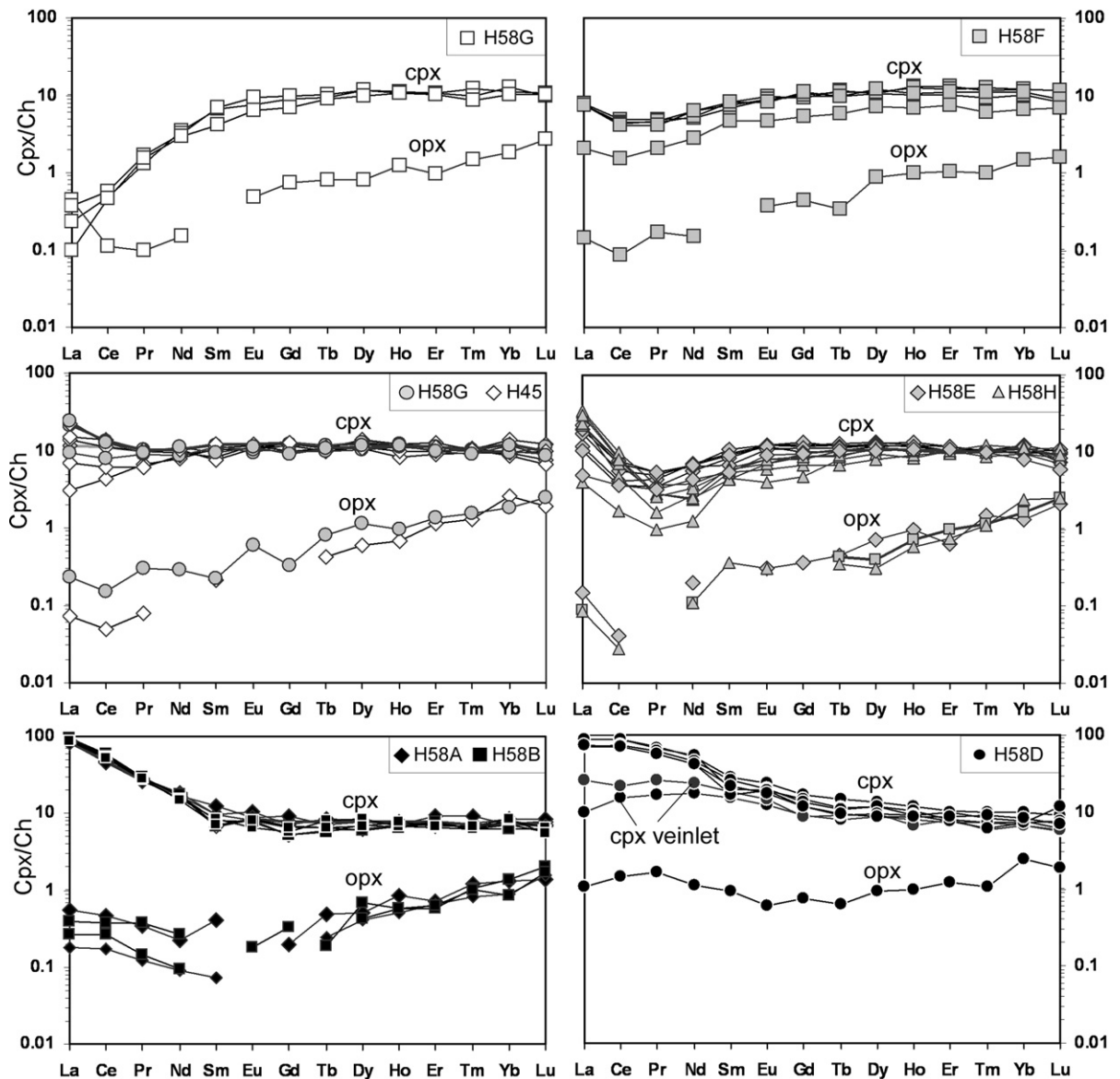


Fig. 5. Chondrite-normalized REE patterns for clinopyroxenes and orthopyroxene from Manazas lherzolite xenoliths. Normalizing factors after Sun and McDonough (1989).

chondrite. Since the HREE in spinel peridotites are mainly hosted in clinopyroxene (Bedini and Bodinier, 1999), these patterns are inversely correlated with the various degree of depletion observed in the different samples. On the other hand, light (L) REE enrichment with  $La_N/Yb_N$  up to 8.3,  $Ce_N/Yb_N$  up to 6.2 and  $Nd_N/Yb_N$  up to 4 characterizes the most depleted samples H58A, H58B and H58D suggesting a direct correlation between mantle depletion and metasomatic enrichment. This is commonly observed in mantle xenoliths worldwide and is experimentally attributed to the more effective permeability of refractory (cpx-poor) peridotite

matrix to metasomatising agents (Toramaru and Fujii, 1986). Accordingly, in the least depleted xenoliths the degree of metasomatic enrichment is less intensive and generally restricted to the lightest REE ( $La_N/Yb_N < 3$ ,  $Ce_N/Yb_N < 1.3$  and  $Nd_N/Yb_N < 1$ ).

### 3. Pyroxene trace element composition

Representative trace element analyses of constituent pyroxenes (opx and cpx) are reported in Table 3 in Appendix A of the online supplement and analytical methods in Appendix B. REE chondrite-normalized

patterns are shown in Fig. 5 and Primordial mantle-normalized incompatible element distributions are available in the online supplement (Appendix C).

Coherently with the REE bulk rock data, the averaged HREE distribution of clinopyroxene decreases from  $10.4\text{--}11.2\times$  chondrite at 10–12% of modal cpx to  $6.9\text{--}8.5\times$  chondrite at 8–9% of modal cpx. Excluding sample H58G, which shows a severe LREE depletion, all samples display variable LREE enrichment that is plausibly induced by metasomatic processes. In samples containing 10–12% modal cpx this enrichment is restricted to the lightest (more incompatible) REE, i.e. La and Ce, thus displaying spoon-shape patterns with  $\text{La}_N/\text{Yb}_N$  up to 3,  $\text{Ce}_N/\text{Yb}_N$  up to 1.6, and  $\text{Nd}_N/\text{Yb}_N$  up to 1.2. Samples characterized by lower modal cpx (8–9%), such as H58A, H58B and H58D, show the highest LREE enrichments with  $\text{La}_N/\text{Yb}_N$  up to 14.6,  $\text{Ce}_N/\text{Yb}_N$  up to 11.9, and  $\text{Nd}_N/\text{Yb}_N$  up to 7.1.

The chondrite-normalized REE distribution in orthopyroxene (Fig. 5) is generally characterized by HREE negative fractionation ( $\text{Tb}_N/\text{Yb}_N$  0.1–0.4). LREE patterns are often upward concave with  $\text{La}_N/\text{Nd}_N$  varying from 0.6 to 3 and generally mimic, at lower level, those of the coexisting clinopyroxene.

In H58D, the REE patterns of clinopyroxene are variable from nearly flat to LREE enriched. The lowest LREE patterns, intermediate between those of clinopyroxene and orthopyroxene, have been observed in a cpx-rich (equigranular textured) veinlet at the boundary with orthopyroxene. This can be interpreted as evidence of clinopyroxene neo-crystallization at the expense of orthopyroxene by metasomatic reaction under conditions of high Ca activity.

Depletion and enrichment processes in mantle parageneses can be successfully evaluated using clinopyroxene REE patterns, since these processes are effectively traced by HREE and LREE distributions, respectively. Application of the model proposed by Johnson et al. (1990) shows that, starting from a common initial mantle source in the spinel stability field (modal cpx: 20%; initial clinopyroxene,  $\text{Cpx}_0$ :  $\text{Yb}_N=14$ ,  $\text{Nd}_N/\text{Yb}_N=1.03$ ), fractional melting of  $\sim 8\%$  could account for the H58H and H58G (modal cpx 11%) clinopyroxene compositions (Fig. 6). Lherzolites H58C, H58E, H58F, and H45 (modal cpx 10–12%) probably suffered similar melting degrees but depart from partial melting trends delineating a progressive  $\text{Nd}_N/\text{Yb}_N$  increase due to slight metasomatic enrichment. The remaining cpx compositions from the most depleted lherzolites (H58A, H58B and H58D) require greater degrees of partial melting (up to 15–20%) which is consistent with their most depleted composition (modal cpx 8–9%) and show the highest metasomatic enrichments ( $\text{Nd}_N/\text{Yb}_N$  up to 7). This confirms that the most depleted cpx-poor peridotite domains were more effectively infiltrated by metasomatising melts in agreement with experimental evidence of melt connectivity in mantle rocks (Toramaru and Fujii, 1986).

Trace element modelling to constrain the metasomatising agent(s) has been performed using partition coefficients (Kd) for clinopyroxene/alkaline basic melts (Zack and Brumm, 1998) and is illustrated in Fig. 7. Calculations have been carried out for the most homogeneously enriched clinopyroxene compositions (samples H58A, H58B and H58D) where it can be assumed that mineral/

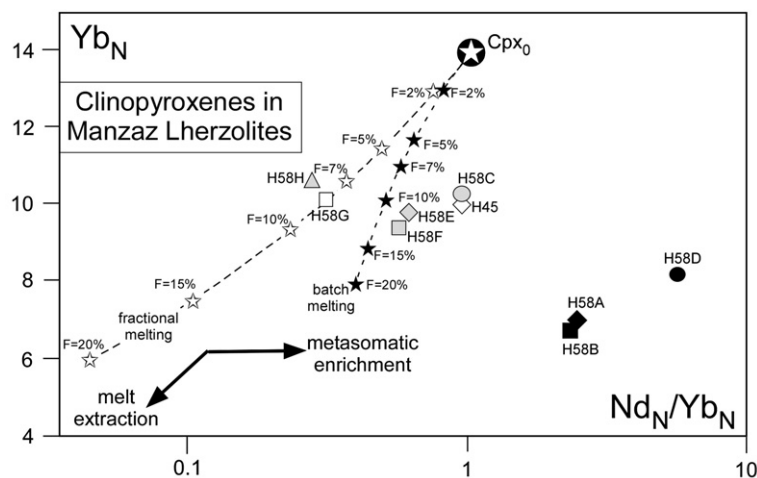


Fig. 6. (a)  $\text{Yb}_N$  vs.  $\text{Nd}_N/\text{Yb}_N$  diagram for clinopyroxene from Manzaz lherzolites. Depletion trends and melting degrees by batch and fractional melting are calculated starting from  $\text{Cpx}_0$  initial source after Bianchini et al. (2007). Lherzolites with 10–12% of modal cpx may reflect less than 12% melting with no or slight metasomatic enrichments; lherzolites with 8–9% of modal cpx (H58A, H58B, H58D) may correspond to higher melting degrees and remarkable metasomatic enrichments. Chondrite normalizing factors are from Sun and McDonough (1989).

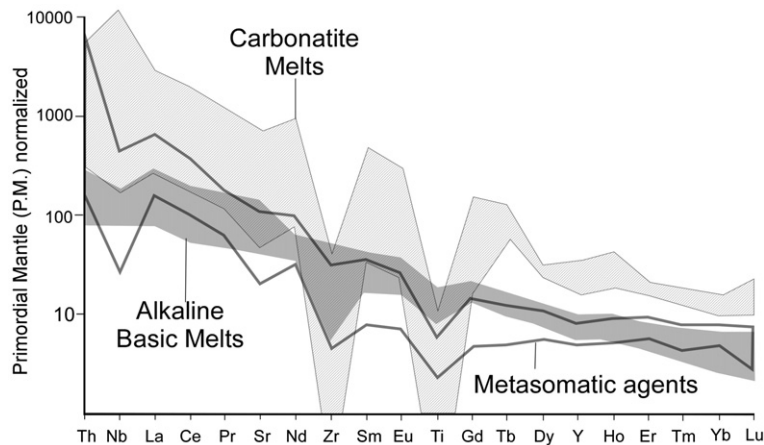


Fig. 7. Primordial Mantle (PM)-normalized trace element patterns of the computed metasomatic agents that affected mantle xenoliths from the Manzaz district. Calculations were performed on the metasomatised clinopyroxene compositions, using distribution coefficients  $cpx/alkaline\ melt$  after Zack and Brumm (1998). Compositional envelopes of alkaline basic melts from the African plate (basanites, nephelinites, melilitites (Azzouni-Sekkal et al., 2007; Beccaluva et al., 1998; Bianchini et al., 1998; Janney et al., 2002)) and carbonatites (Nelson et al., 1998; Coltorti et al., 1993; Smithies and Marsh, 1998) are reported for comparison. Normalizing factors after Sun and McDonough (1989).

melt equilibrium was approached. Comparison with compositional fields of natural alkaline basic volcanics and carbonatites reveals that the inferred metasomatic agent(s) can be best equated with alkali-silicate melts such as alkali-basalts, basanites and melilitites from the African plate (Azzouni-Sekkal et al., 2007; Beccaluva et al., 1998; Bianchini et al., 1998; Janney et al., 2002). However, discrepancies are evident in the deficiency of Ti and excess of Th for some theoretical compositions, thus suggesting that the strongly alkaline metasomatic melts could be also characterized by variable enrichment in carbonatitic components, that in the extreme case could reach a silico-carbonatitic composition. This seems to be confirmed also by the  $La_N/Yb_N$  vs  $Ti/Eu$  diagram (Coltorti et al., 1999) where the most enriched Manzaz cpxs plot between the alkali silicate- and carbonatite-metasomatised clinopyroxene fields (figure in Appendix C of the online supplement). The above conclusions agree with those of Grégoire et al. (2000) and Delpéch et al. (2004) for Kerguelen mantle xenoliths that are interpreted to have been affected by carbonate-rich silicate melts rather than pure carbonatites. They also conform with findings reported by (Dautria et al., 1992) for peridotite xenoliths collected at In Teria (NE Hoggar margin) that emphasised the alkali-silicate to carbonatite nature of the metasomatising agents.

#### 4. Isotope characteristics of the Manzaz mantle xenoliths

Cpx separates from the Manzaz xenoliths have  $^{87}Sr/^{86}Sr=0.70214-0.70323$ ,  $^{143}Nd/^{144}Nd=0.51295-$

$0.51366$ ,  $^{206}Pb/^{204}Pb=19.52-20.18$ ,  $^{207}Pb/^{204}Pb=15.66-15.72$ ,  $^{208}Pb/^{204}Pb=38.62-39.93$  (Table 4 in Appendix A of the online supplement; analytical methods in Appendix B). For both whole-rock and clinopyroxene,  $Nd_N/Yb_N$  ratios are inversely correlated with  $^{143}Nd/^{144}Nd$ , with the higher isotopic ratios recorded in samples containing 10–12% modal cpx (i.e. least affected by metasomatism) and the lower values recorded in samples with lowest modal cpx (8–9%) which appear more effectively metasomatised. This confirms that the permeability of the peridotite matrix, related to its clinopyroxene content (Toramaru and Fujii, 1986), also influences the mantle isotopic fingerprint.

In the Sr vs. Nd isotope diagram (Fig. 8), the samples with 10–12% modal cpx plot in the upper-left quadrant close to the depleted mantle (DM) end-member, whereas those with 8–9% modal cpx cluster around the HIMU mantle end-member ( $^{87}Sr/^{86}Sr=0.7031-0.7032$ ,  $^{143}Nd/^{144}Nd=0.51292-0.51295$ ). The HIMU Sr–Nd isotope composition can be considered the predominant signature of the metasomatic agents. The HIMU fingerprint is also recorded in the Hoggar alkaline lavas (Allègre et al., 1981) and, more in general, in all the North Africa Cenozoic alkaline lavas (Jebel Marra (Davidson and Wilson, 1989; Franz et al., 1999); Gharyan district (Beccaluva et al., in press); Iblean and Sicily Channel districts (Bianchini et al., 1998; Civetta et al., 1998), and therefore it can be considered as a ubiquitous component that affected the lithosphere on a regional scale.

Lead isotopes, while unequivocally confirming the HIMU signature of the metasomatising agent, also

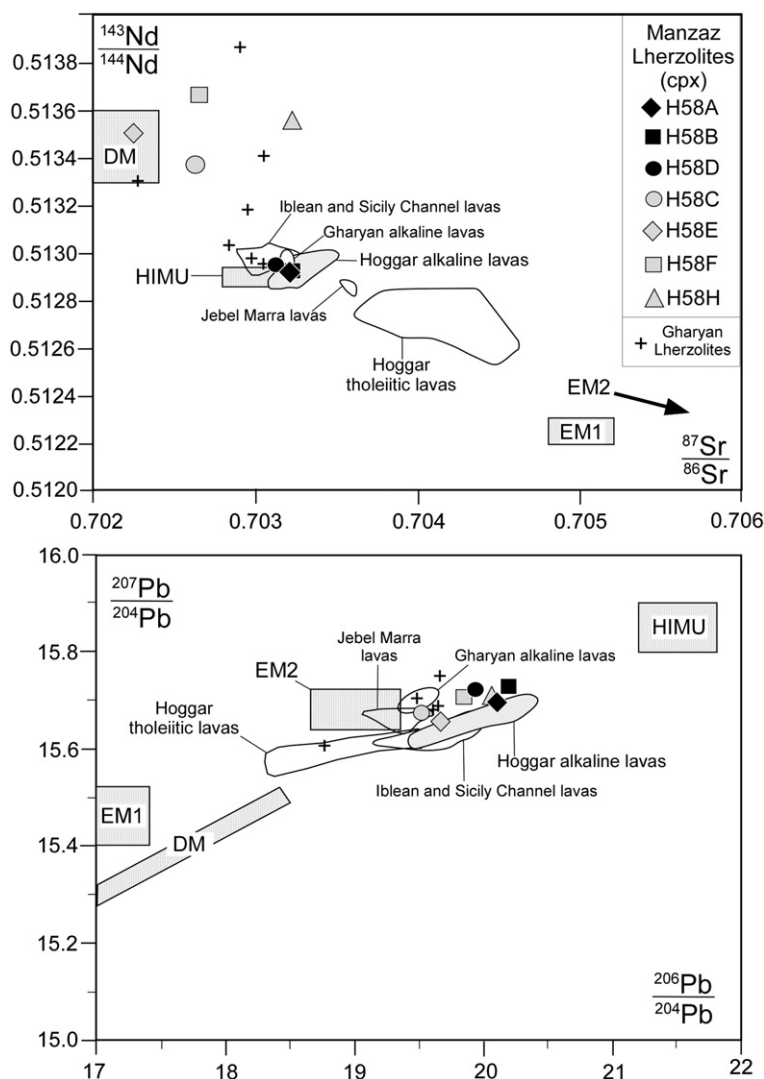


Fig. 8. Sr–Nd–Pb isotopic variations for clinopyroxenes from Manzaz mantle xenoliths. Composition of mantle xenoliths from the Gharyan district of Libya (Beccaluva et al., *in press*), and Cenozoic alkaline lavas from various African volcanic districts are reported for comparison: Hoggar (Allège et al., 1981); Jebel Marra (Davidson and Wilson, 1989; Franz et al., 1999); Iblean–Sicily Channel Districts (Beccaluva et al., 1998; Bianchini et al., 1998; Civetta et al., 1998). Isotopic mantle end members (DM, HIMU, EM1 and EM2) are reported after Zindler and Hart (1986).

display a clear decoupling with respect to Sr–Nd isotopes in the least metasomatised samples. In fact, the enrichment in  $^{206}\text{Pb}$  ( $^{206}\text{Pb}/^{204}\text{Pb}=19.5\text{--}20.1$ ) and  $^{208}\text{Pb}$  ( $^{208}\text{Pb}/^{204}\text{Pb}=38.6\text{--}39.8$ ) is significant even in samples H58C, H58E, H58F, H58H that are considered largely unaffected by metasomatism on the basis of  $^{143}\text{Nd}/^{144}\text{Nd}$  (0.51337–0.51366). This apparent incongruence between the Sm–Nd and the U–Pb systems has also been observed in the Gharyan mantle xenoliths (Beccaluva et al., *in press*) and may be attributed to the greater mobility of Pb compared to Nd (and Sr), as indicated by the respective cpx/melt partition coefficients (Geochemical Earth Reference Model (GERM)) Staudigel et al., 1998. Therefore

Pb isotopes appear to be more sensitive indicators of incipient metasomatic reactions.

The very high  $^{143}\text{Nd}/^{144}\text{Nd}$  of H58E, H58F, H58H ( $>0.5135$ ) suggests that the relative mantle domains were affected by pre-Paleozoic partial melting events in the presence of residual garnet resulting in high Sm/Nd that ultimately led to the very high Nd isotopic ratios (Downes et al., 2003; Bianchini et al., 2007). This implies that these mantle rocks were subsequently re-equilibrated at a lower depth in the current spinel stability facies. Significantly, garnet-bearing lherzolites have been reported in mantle xenolith population of In Teria volcanic district (NE Hoggar margin (Dautria et al., 1992)).

A helium isotope determination has been made on gas from inclusions trapped in olivine from the metasomatised lherzolite H58B and gave  $^3\text{He}/^4\text{He}$  of 6.6 Ra (where Ra is the atmospheric composition  $1.39 \times 10^{-6}$ ). Although the measured value is slightly lower than several Hoggar lavas (Pik et al., 2006), similar ratios are recorded in Cenozoic HIMU-related products from the northern-central African lithosphere, e.g. peridotite xenoliths from the Gharyan (Beccaluva et al., *in press*) and Iblean volcanic districts (Sapienza et al., 2005), as well as alkaline lavas from Etna (Marty et al., 1994), Cameroon Line (Barfod et al., 1999) and Canaries (Hilton et al., 2000). Indeed, they are consistent with the rather uniform  $^3\text{He}/^4\text{He}$  that characterizes HIMU volcanism irrespective of the strength of Pb isotopes and trace element ratio signal.

## 5. Discussion and conclusions

Most peridotite xenoliths from the Manzas volcanic district record metasomatic enrichment that overprinted a previously depleted mantle lithosphere. Trace element modelling of the metasomatised clinopyroxenes allows us to infer that the metasomatising agents were highly alkaline carbonated melts such as nephelinites/melilitites (or at their most extreme silico-carbonatites). They are characterized by a clear HIMU Sr–Nd–Pb–He isotopic signature.

In some cases there is a decoupling of Nd–Sr and Pb isotopes. This may be explained by a greater mobility of Pb (U, Th, La, Ce) that could be modelled by chromatographic fractionation processes as proposed by Bodinier et al. (2004). This decoupling is evident in xenoliths containing more than 9% cpx, implying that below this “petrological barrier”, a coherent metasomatic imprint for all isotopes is attained due to higher permeability in the most refractory (cpx-poor) peridotite domains (Toramaru and Fujii, 1986), where a sufficiently high metasomatic melt/matrix ratio occurs.

The Sr–Nd–Pb isotope composition typical of EM1-type enriched mantle, that is observed for the older tholeiitic plateau basalts of Hoggar (Aït-Hamou et al., 2000), does not appear to be represented in the lithospheric mantle sampled by the xenoliths. Since the EM1 signature can originate as an old component of the Pan–African lithosphere (Cottin et al., 1998; Aït-Hamou et al., 2000), its absence in mantle xenoliths (and the associated alkaline lavas) is perplexing. This cannot be attributed to a deeper provenance of mantle xenoliths with respect to the EM1 mantle portions where tholeiitic basalts were originated, owing to their comparable depth range of origin (1–2 GPa (Green and Fallon, 2005)).

More convincing explanations involve the lateral displacement of an old lithospheric mantle by upwelling asthenosphere from the underlying convective mantle. The resulting “rejuvenated” lithosphere may represent a single mantle column from which both basic alkaline melts could have been produced at deeper depths, and mantle xenoliths have been sampled at shallower levels. This is supported by the interpretation of the mantle xenoliths as garnet (gt)-bearing mantle domains re-equilibrated to spinel lherzolites in accordance with the high  $^{143}\text{Nd}/^{144}\text{Nd}$  observed in several samples. Garnet (and spinel) peridotite xenoliths have been found in the In Teria volcanic district along the NE Hoggar margin (Dautria et al., 1992), which plausibly represents the older cratonic lithospheric mantle. Significantly, the In Teria spinel peridotite xenoliths record widespread pyrometamorphic textures (secondary aggregates of olivine, clinopyroxene, spinel and feldspar essentially formed from primary orthopyroxene and spinel (Dautria et al., 1992)) that testify to reactions with metasomatic melts at shallow mantle depths, probably in the more rigid mechanical boundary layer. Similar reaction textures are also recorded in mantle xenoliths from other volcanic districts of the North African belt (Iblei, Sicily (Beccaluva et al., 2005); Gharyan, Libya (Beccaluva et al., *in press*)) but have not been observed in the Manzas xenoliths in which metasomatism seems to be texturally re-equilibrated. This probably means that metasomatic reactions beneath the central Hoggar occurred at comparatively greater depth, i.e. in the thermal boundary layer, prior and/or during mantle uprising. It is conceivable that at these depths, higher temperatures and more effective elemental diffusion could have facilitated re-equilibration processes preventing the formation/persistence of pyrometamorphic textures.

The Manzas spinel–lherzolites could be interpreted as representative of an upwelling asthenospheric mantle diapir that accreted to the older cratonic lithosphere. Relics of the cratonic lithosphere are probably represented by the variably metasomatised garnet- to spinel–peridotite xenoliths recovered at In Teria (Fig. 9). These mantle dynamics certainly contributed to lithosphere bulging that resulted in the Hoggar swell, and are consistent with the geophysical evidence such as the gravity field data (–90 mgal (Lesquer et al., 1988)) and the thermal anomaly centred on the Atakor volcanism (heat flow  $63 \text{ mW/m}^2$  (Lesquer et al., 1989)). Recent fission track age data suggest that the regional uplift of the Hoggar basement started at least as early as the Cretaceous (Khaldi et al., 2006). Seismic tomography of the North African plate confirms a variable lithospheric thickness in the Saharan area due to local asthenospheric upwelling (Ayadi et al., 2000), but seems to rule out the

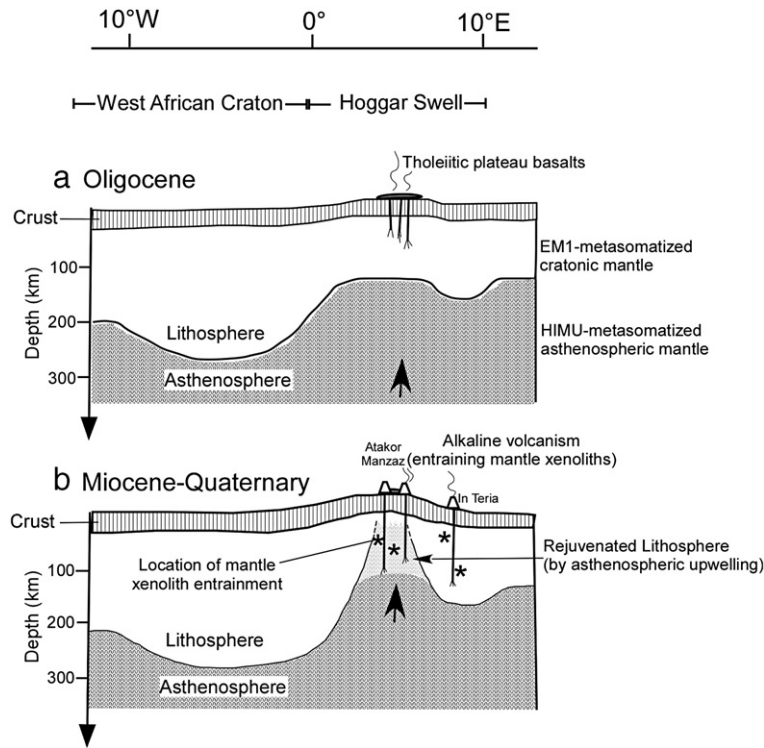


Fig. 9. Simplified cartoon showing the hypothesised lithosphere/asthenosphere interaction beneath the Hoggar swell. (a) Tholeiitic plateau basalts (35–30 Ma, Anahef district) formed by high melting degrees of EM1-metasomatized mantle of the Pan–African cratonic lithosphere. (b) Younger alkaline volcanism of the Atakor–Manzaz district generated from low melting degrees of HIMU-metasomatized mantle sources. The latter probably represent a rejuvenated lithosphere formed by intra-cratonic upwelling and accretion of asthenospheric material. The Manzaz spinel lherzolite xenoliths may therefore represent fragments of this rejuvenated lithosphere, whereas the garnet/spinel peridotite xenoliths from In Teria may represent the older cratonic mantle of the Pan–African lithosphere.

existence of deep mantle plumes (Davaille et al., 2005; Sebai et al., 2006).

The systematic occurrence of Neogene alkaline lavas and associated mantle xenoliths with a clear HIMU affinity across the African plate indicates that it is a ubiquitous sub-lithospheric component across Central-Northern Africa. The widely accepted genetic interpretation of the HIMU end-member may fit with the framework delineated above. In fact this component is considered related to the ultimate fate of subducted oceanic lithotypes which create high U/Pb and Th/Pb mantle domains that, after a long-term storage, result in highly radiogenic Pb compositions (Weaver, 1991; Carlson, 1995; Hofmann, 1997). Accordingly, Wilson and Patterson (2001) physically locate this component above the 670 km discontinuity in the upper mantle, where geophysical evidence shows subducted slab relics flattened over wide upper mantle regions (e.g. in the Central Mediterranean (Faccenna et al., 2001)).

Helium isotopes carried out on Cenozoic volcanics and associated mantle xenoliths across Central-Northern

Africa ( $R_a < 9$ ; (Beccaluva et al., in press; Pik et al., 2006)) also corroborate the interpretation of HIMU as a common regional sub-lithospheric component. The relatively low  $^3\text{He}/^4\text{He}$  ratios observed for the Saharan districts represent a further indication that this metasomatic component is confined in the upper mantle, unlike the Ethiopian–Yemen plateau basalts ( $^3\text{He}/^4\text{He}$  up to 20  $R_a$ ) which have been related to a deep mantle plume possibly generated from the core–mantle boundary (Pik et al., 2006)). By contrast, relatively low  $^3\text{He}/^4\text{He}$  can be satisfactorily explained by degassing of shallow mantle domains and/or the addition of recycled components to the upper mantle (Moreira and Kurz, 2001).

In conclusion, convection within the upper mantle and lithosphere/asthenosphere interactions taking place mainly along lithospheric discontinuities such as craton/mobile belt borders, as proposed by the edge-driven convection model (King and Anderson, 1995; King and Anderson, 1998), can be considered the most appropriate geodynamic scenario for the mantle evolution of the Hoggar swell. Whatever the complex terminology of the

convective instabilities in the mantle, referred to various types of plumes and hot-spots (Courtilot et al., 2003), the geochemistry of the Hoggar xenoliths seems to be satisfactorily accounted for by shallow convective processes with the origin of the related geochemical components confined within the upper mantle. Therefore, the Hoggar volcanism, as well as other volcanic occurrences of the Saharan belt, are likely to be related to passive asthenospheric mantle uprising and its decompression melting linked to tensional stresses in the lithosphere during tectonic reactivation and rifting of the Pan–African basement. This can be considered a far-field foreland reaction of the Africa–Europe collisional system operational since the Eocene (Azzouni-Sekkal et al., 2007; Liégeois et al., 2005).

### Acknowledgements

The authors gratefully acknowledge the constructive criticism of M. Grégoire and of an anonymous referee that greatly improved the manuscript. Particular thanks are extended to R. Carlson for his suggestions and encouragement. The SUERC laboratories are supported by the Scottish Universities.

### Appendix A. Supplementary data

Supplementary data associated with this article can be found, in the online version, at [doi:10.1016/j.epsl.2007.05.047](https://doi.org/10.1016/j.epsl.2007.05.047).

### References

- Aït-Hamou, F., Dautria, J.M., Cantagrel, J.M., Dostal, J., Briquieu, L., 2000. Nouvelles données géochronologiques et isotopiques sur le volcanisme cénozoïque de l'Ahaggar (Sahara algérien): des arguments en faveur d'un panache. *Comptes Rendus de l'Académie des Sciences de Paris* 330, 829–836.
- Allègre, C.J., Dupré, B., Lambert, B., Richard, P., 1981. The sub-continental versus sub-oceanic debate. Lead–neodymium–strontium isotopes in primary basalts in a shield area: the Ahaggar volcanic suite. *Earth Planet. Sci. Lett.* 52, 85–92.
- Ayadi, A., Dorbath, C., Lesquer, A., Bezzeghoud, M., 2000. Crustal and upper mantle velocity structure of the Hoggar swell (Central Sahara, Algeria). *Phys. Earth Planet. Inter.* 118, 111–123.
- Azzouni-Sekkal, A., Bonin, B., Benhallou, A., Yahiaoui, R., Liégeois, J.-L., 2007. Tertiary alkaline volcanism of the Atakor Massif (Hoggar, Algeria). In: Beccaluva, L., Bianchini, G., Wilson, M. (Eds.), “Cenozoic volcanism in the Mediterranean Area”. Geological Society of America (GSA) Special Paper, 418, pp. 321–340.
- Beccaluva, L., Siena, F., Coltorti, M., Di Grande, A., Lo Giudice, A., Macciotta, G., Tassinari, R., Vaccaro, C., 1998. Nephelinitic to tholeiitic magma generation in a transtensional tectonic setting: an integrated model for the Iblean volcanism, Sicily. *J. Petrol.* 39, 1547–1576.
- Beccaluva, L., Bianchini, G., Bonadiman, C., Coltorti, M., Macciotta, G., Siena, F., Vaccaro, C., 2005. Within-plate Cenozoic volcanism and lithospheric mantle evolution in the western-central Mediterranean area. In: Finetti, I. (Ed.), Elsevier Special Volume, Crop Project — Deep Seismic Exploration of the Central Mediterranean and Italy, pp. 641–664.
- Beccaluva, L., Bianchini, G., Ellam, R.M., Marzola, M., Oun, K.M., Siena, F., Stuart, F.M. The role of HIMU metasomatic components in the African lithospheric mantle: petrological evidence from the Gharyan peridotite xenoliths, NW Libya, in Coltorti, M., Grégoire, M. (Eds.) “Mantle metasomatism in intra-plate and suprasubduction settings”, Geological Society, Special Publication, in press.
- Bedini, R.M., Bodinier, J.-L., 1999. Distribution of incompatible trace elements between the constituents of spinel peridotite xenoliths: ICP-MS data from the East African Rift. *Geochim. Cosmochim. Acta* 63, 3883–3900.
- Bianchini, G., Clocchiatti, R., Coltorti, M., Joron, J.L., Vaccaro, C., 1998. Petrogenesis of mafic lavas from the northernmost sector of the Iblean District (Sicily). *Eur. J. Mineral.* 10, 301–315.
- Bianchini, G., Beccaluva, L., Bonadiman, C., Nowell, G., Pearson, G., Siena, F., Wilson, M., 2007. Evidence of distinct depletion and metasomatic processes in harzburgite–lherzolite mantle xenoliths from the Iberian lithosphere (Olot, NE Spain). *Lithos* 94, 25–45.
- Barfod, D., Ballentine, C.J., Halliday, A.N., Fitton, J.G., 1999. Noble gases in the Cameroon line and the He, Ne and Ar isotopic compositions of high  $\mu$  (HIMU) mantle. *J. Geophys. Res.* 104, 29509–29527.
- Bodinier, J.L., Menzies, M.A., Shimizu, N., Frey, F.A., McPherson, E., 2004. Silicate, hydrous and carbonate metasomatism at Lherz, France: contemporaneous derivatives of silicate melt–harzburgite reaction. *J. Petrol.* 45, 299–320.
- Brey, G.P., Köhler, T.P., 1990. Geothermobarometry in four phases lherzolites II. New thermobarometers and practical assessment of existing thermobarometers. *J. Petrol.* 31, 1353–1378.
- Carlson, R.W., 1995. Isotopic inferences on the chemical structure of the mantle. *J. Geodyn.* 20, 365–386.
- Civetta, L., D’Antonio, M., Orsi, G., Tilton, G.R., 1998. The geochemistry of volcanic rocks from Pantelleria island, Sicily Channel: petrogenesis and characteristics of the mantle source region. *J. Petrol.* 39, 1453–1492.
- Coltorti, M., Alberti, A., Beccaluva, L., Dos Santos, A.B., Mazzucchelli, M., Morais, E., Rivalenti, G., Siena, F., 1993. The Tchivira–Bonga alkaline–carbonatite complex (Angola): petrological study and comparison with some Brazilian analogues. *Eur. J. Miner.* 5, 1001–1024.
- Coltorti, M., Bonadiman, C., Hinton, R.W., Siena, F., Upton, B.G.J., 1999. Carbonatite metasomatism of the oceanic upper mantle: evidence from clinopyroxenes and glasses in ultramafic xenoliths of Grande Comore, Indian Ocean. *J. Petrol.* 40, 133–165.
- Cottin, J.Y., Lorand, J.P., Agrinier, P., Bodinier, J.L., Liégeois, J.P., 1998. Isotopic (O, Sr, Nd) and trace element geochemistry of the Laoumi layered intrusions (Pan–African belt, Hoggar, Algeria): evidence for post-collisional continental tholeiitic magmas variably contaminated by continental crust. *Lithos* 45, 197–222.
- Courtilot, V., Davaille, A., Besse, J., Stock, J., 2003. Three distinct types of hotspots in the Earth’s mantle. *Earth Planet. Sci. Lett.* 205, 295–308.
- Dautria, J.M., Dupuy, C., Takherist, D., Dostal, J., 1992. Carbonate metasomatism in the lithospheric mantle: peridotitic xenoliths from a melilititic district of the Sahara basin. *Contrib. Mineral. Petrol.* 111, 37–52.

- Davaille, A., Stutzmann, E., Silveira, G., Besse, J., Courtillot, V., 2005. Convective patterns under the Indo-Atlantic « box ». *Earth Planet. Sci. Lett.* 239, 233–252.
- Davidson, J.P., Wilson, I.R., 1989. Evolution of an alkali basalt–trachyte suite from Jebel Marra volcano, Sudan, through assimilation and fractional crystallization. *Earth Planet. Sci. Lett.* 95, 141–160.
- Delpech, G., Grégoire, M., O'Reilly, S.Y., Cottin, J.Y., Moine, B., Michon, G., Giret, A., 2004. Feldspar from carbonate-rich silicate metasomatism in the shallow oceanic mantle under Kerguelen Islands (South Indian Ocean). *Lithos* 75, 209–237.
- Downes, H., Reichow, M.K., Mason, P.R.D., Beard, A.D., Thirlwall, M.F., 2003. Mantle domains in the lithosphere beneath the French Massif Central: trace element and isotopic evidence from mantle clinopyroxenes. *Chem. Geol.* 200, 71–87.
- Faccenna, C., Funicello, F., Giardini, D., Lucente, P., 2001. Episodic back-arc extension during restricted mantle convection in the Central Mediterranean. *Earth Planet. Sci. Lett.* 187, 105–116.
- Franz, G., Steiner, G., Volker, F., Pudlo, D., Hammerschmidt, K., 1999. Plume related alkaline magmatism in central Africa — the Meidob Hills (W Sudan). *Chem. Geol.* 157, 27–47.
- Green, D.H., Fallon, T.J., 2005. Primary magmas at mid-ocean ridges, “hotspots,” and other intraplate settings: constraints on mantle potential temperature. In: Foulger, G.R., Natland, J.H., Presnall, D. C., Anderson, D.L. (Eds.), *Plates, Plumes and Paradigms*. Geological Society of America (GSA) Special Paper, vol. 388, pp. 217–247.
- Grégoire, M., Moine, B.N., O'Reilly, S.Y., Cottin, J.Y., Giret, A., 2000. Trace element residence and partitioning in mantle xenoliths metasomatised by highly alkaline, silicate-and carbonate-rich melts (Kerguelen Islands, Indian Ocean). *J. Petrol.* 41, 477–509.
- Hilton, D.R., McPherson, C.G., Elliot, T.R., 2000. Helium isotope ratios in mafic phenocryst and geothermal fluids from La Palma, the Canary Islands (Spain): implications for HIMU mantle source. *Geochim. Cosmochim. Acta* 64, 2119–2132.
- Hofmann, A.W., 1997. Mantle geochemistry: the message from oceanic volcanism. *Nature* 385, 219–229.
- Janney, P.E., Le Roex, A.P., Carlson, R.W., Viljoen, K.S., 2002. A chemical and multi-isotope study of the Western Cape Olivine Melilitite Province, South Africa: implications for the sources of kimberlites and the origin of the HIMU signature in Africa. *J. Petrol.* 43, 2339–2370.
- Jaques, A.L., Green, D.H., 1980. Anhydrous melting of peridotite at 0–15 kb pressure and the genesis of tholeiitic basalts. *Contrib. Mineral. Petrol.* 73, 13–27.
- Johnson, K.T., Dick, H.J.B., Shimizu, N.N., 1990. Melting in the oceanic upper mantle: an ion microprobe study of diopsides in abyssal peridotites. *J. Geophys. Res.* 95, 2661–2678.
- Khaldi, A., Nacer, J.-E., Badani, A., Van Der Beek, P., Labrin, E., Chahdane, R., Bentchakal, M., 2006. Age trace de fission Crétacé Inférieur du plissement à grand rayon de courbure du Hoggar (Sahara Central, Algérie). Abstracts book of the 4th International Geological Correlation Program IGCP-485 (Algiers, December 2006), p. 15.
- King, S.D., Anderson, D.L., 1995. An alternative mechanism of flood basalt formation. *Earth Planet. Sci. Lett.* 136, 269–279.
- King, S.D., Anderson, D.L., 1998. Edge-driven convection. *Earth Planet. Sci. Lett.* 160, 289–296.
- Lesquer, A., Bourmatte, A., Dautria, J.M., 1988. Deep structure of the Hoggar domal uplift (Central sahara, south Algeria) from gravity thermal and petrological data. *Tectonophysics* 152, 71–87.
- Lesquer, A., Bourmatte, A., Ly, S., Dautria, J.M., 1989. First heat flow determination from the Central Sahara: relationships with the Pan-African belt and Hoggar domal uplift. *J. Afr. Earth Sci.* 9, 41–48.
- Liégeois, J.P., Benhallou, A., Azzouni-Sekkal, A., Yahiaoui, R., Bonin, B., 2005. The Hoggar swell and volcanism: reactivation of the Precambrian Tuareg shield during Alpine convergence and West African Cenozoic volcanism. In: Foulger, G.R., Natland, J.H., Presnall, D.C., Anderson, D.L. (Eds.), *Plates, Plumes and Paradigms*. Geological Society of America (GSA) Special Paper, vol. 388, pp. 379–400.
- Marty, B., Trull, T., Lussiez, P., Basile, I., Tanguy, J.-C., 1994. He, Ar, O, Sr and Nd isotope constraints on the origin and evolution of Mount Etna magmatism. *Earth Planet. Sci. Lett.* 126, 23–39.
- Moreira, M., Kurz, M.D., 2001. Subducted oceanic lithosphere and the origin of the ‘high  $\mu$ ’ basalt helium isotopic signature. *Earth Planet. Sci. Lett.* 189, 49–57.
- Mysen, B.O., Kushiro, I., 1977. Compositional variations of coexisting phases with the degree of melting of peridotite in the upper mantle. *Am. Mineral.* 62, 843–865.
- Nelson, D.R., Chivas, A.R., Chappell, B.W., McCulloch, M.T., 1998. Geochemical and isotopic systematics in carbonatites and implications for the evolution of ocean island sources. *Geochim. Cosmochim. Acta* 52, 1–17.
- Niu, Y., 1997. Mantle melting and melt extraction processes beneath ocean ridges: evidence from abyssal peridotites. *J. Petrol.* 38, 1047–1074.
- Pik, R., Marty, B., Hilton, D.R., 2006. How many plumes in Africa? The geochemical point of view. *Chem. Geol.* 226, 100–114.
- Raffone, N., Zanetti, A., Chazot, G., Deniel, C., Vannucci, R., 2001. Geochemistry of Mantle Xenoliths from Ibalrhate (Mid Atlas, Morocco): Insights into the Lithospheric Mantle Evolution During Continental Rifting, 11th Goldschmidt Conference. Hots Springs, (U.S.A.).
- Raffone, N., Zanetti, A.M., Chazot, G., Pin, C., Vannucci, R. Multiple steps of melt percolation through lithospheric mantle recorded by REE and HFSE zoning in cpx and amph of wehrlites from Azrou (mid Atlas, Morocco). 32nd IGC (2004) Florence.
- Sapienza, G., Hilton, D.R., Scribano, V., 2005. Helium isotopes in peridotite mineral phases from Hyblean Plateau xenoliths (southeastern Sicily, Italy). *Chem. Geol.* 219, 115–129.
- Sebai, A., Stutzmann, E., Montagner, J.-P., Sicilia, D., et al., 2006. Anisotropic structure of the African upper mantle from Rayleigh and Love wave tomography. *Phys. Earth Planet. Inter.* 155, 48–62.
- Smithies, R.H., Marsh, J.S., 1998. The Marinkas Quellen carbonatite complex, Southern Namibia; carbonatite magmatism with an uncontaminated depleted mantle signature in a continental setting. *Chem. Geol.* 148, 201–212.
- Staudigel, H., Albarède, F., Blichert-Toft, J., Edmond, J., McDonough, B., et al., 1998. Geochemical Earth Reference Model (GERM): description of the initiative. *Chem. Geol.* 145, 153–159.
- Sun, S.-S., McDonough, W.F., 1989. Chemical and isotopic systematics of oceanic basalts: implications for mantle composition and process, Chemical and isotopic systematics of oceanic basalts: implications for mantle composition and process. In: Saunders, A.D., Norry, M.J. (Eds.), *Magmatism in the Oceanic Basins*. Geological Society, Special Publication, vol. 42, pp. 313–346.
- Toramaru, A., Fujii, N., 1986. Connectivity of melt phase in a partially molten peridotite. *J. Geophys. Res.* 91, 9239–9252.
- Weaver, B.L., 1991. The origin of ocean island basalt end-member compositions: trace element and isotopic constraints. *Earth Planet. Sci. Lett.* 104, 381–397.

- Wilson, M., Patterson, R., 2001. Intraplate magmatism related to short-wavelength convective instabilities in the upper mantle: evidence from the Tertiary–Quaternary volcanic province of Western and Central Europe. In: Ernst, R.E., Buchan, K.L. (Eds.), *Mantle Plumes: Their Identification Through Time*. Geological Society of America (GSA) Special Paper, vol. 352, pp. 37–58.
- Zack, T., Brumm, R., 1998. Ilmenite/liquid partition coefficients of 26 trace elements determined through ilmenite/clinopyroxene partitioning in garnet pyroxenites. 7th International Kimberlite Conference. Cape Town, pp. 986–988.
- Zindler, A., Hart, S.R., 1986. Chemical geodynamics. *Earth and Planetary Sciences. Annual Review*, vol. 14, pp. 493–571.